12

Protein Engineering of PQQ Glucose Dehydrogenase

Satoshi Igarashi and Koji Sode
Tokyo University of Agriculture and Technology Koganei, Tokyo, Japan

1 INTRODUCTION

1.1 PQQ and PQQ-Harboring Enzymes

Pyrroloquinoline quinone (PQQ) was first proposed in the 1960s as the third major prosthetic group (along with pyridine nucleotides and flavins) for redox enzymes (1). After about two decades, the structure of PQQ (Fig. 1) was F1
determined by two groups (2,3). PQQ is the *ortho*-quinone at the C4 and C5 positions of the quinone ring. The C5 carbonyl group in the oxidized form is very reactive towards nucleophiles such as alcohols, sugars, amines, ammonia, cyanide, and amino acids. Knowledge about PQQ in the view of biology, biochemistry, and electrochemistry has been studied and summarized in several reviews (4–12). Until now, many PQQ-harboring proteins or PQQ and heme-harboring proteins have been discovered but only in Gram-negative bacteria (Table 1). Most of the PQQ-harboring enzymes belonged T1
to dehydrogenases (4–31): PQQ methanol dehydrogenases (PQQMDH), PQQ ethanol dehydrogenases (PQQEDH), and PQQ glucose dehydrogenases (PQQGDH).

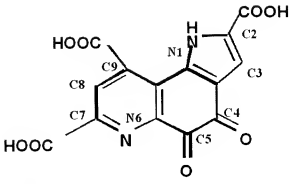

Figure 1 The structure of pyrroloquinoline quinone (PQQ).

PQQMDHs oxidize methanol to formaldehyde during the growth of methylotrophic bacteria on methane or methanol (32–34). PQQMDH from Methylotroph sp. was the first PQQ enzyme for which a tertiary structure was elucidated. PQQMDH is a soluble periplasmic enzyme composed of $\alpha 2\beta 2$ heterotetrameric structure (35). The catalytic subunit, the α-subunit (about 60 kDa), possesses one PQQ molecule and one Ca^{2+} ion. The α-subunit was shown to be an 8-bladed β-propeller fold (36). Other PQQ enzymes also appear to be β-propeller proteins. The β-propeller structure is composed of a repetitive folding unit called the W-motif, which is arranged circularly like the blades of propeller (Fig. 2). The W-motif is composed of four antiparallel β- **F2** strands. β-Propeller proteins having four to eight W-motifs have been reported (37).

PQQ-dependent alcohol dehydrogenases including PQQMDHs can be categorized into three types. The first group named ADH I was soluble alcohol dehydrogenases, including PQQMDH. The difference between PQQMDH and PQQEDH was simply substrate specificity (34). Type I PQQEDHs are homodimers of identical subunit of 60 kDa each, and its structure is 8-bladed β-propeller fold similar to PQQMDHs (38,39). ADH II is classified as heme-possessing PQQADH (15). The overall structure is composed of two domains: the N-terminal domain (1–566) as an 8-bladed β-propeller fold containing one PQQ molecule and one calcium ion in its active site and the C-terminal type I cytochrome domain (591–667) (40). The ADH III is a membrane-bound type alcohol dehydrogenase. ADH III is comprised of three subunits: α (catalytic), β (cytochrome), and small subunit (41,42). The α subunit has one PQQ molecule and single heme C, and β subunit possesses three heme C's. In an electrochemical field, direct electron transfer from PQQ to an electrode via heme C was observed (43). The substrate specificity profile of ADH III is relatively restricted compared with other ADHs (12).

Table 1 The list of PQQ or PQQ-Heme-Harboring Proteins

		Prosthetic group	Location	Component	Organism	Ref.
Alcohol dehydrogenases						
Type I	Methanol dehydrogenase	PQQ	Periplasm	$\alpha_2\beta_2$[2]	Methylotrophs *Paracoccus denitrificans*	4
	Ethanol dehydrogenase	PQQ	Periplasm	Homodimeric	*Pseudomonas* sp.	12
Type II	Alcohol dehydrogenase	PQQ/heme C	Periplasm	Monomeric	*Comamonas testosteroni*	15
					P. putida HK5	16
	Tetrahydrofurfuryl alcohol dehydrogenase	PQQ/ heme C	?	Monomeric	*Ralstonia eutropha* strain B0	17
	Polyvinyl alcohol dehydrogenase	PQQ/ heme C	?	Monomeric	Pseudomonas sp. strain VM15C	18
	Polyethylene glycol dehydrogenase	PQQ/ heme C	?	Tetrameric	*Rhodopseudomonas acidophila*	19
			Periplasm/ membrane-bound		*Flavobacterium* sp.	20
	Polypropylene glycol dehydrogenase	PQQ	Periplasm/ membrane-bound	Homodimeric	*Pseudomonas* sp. *Stenotrophomonas maltophilia*	20
Type III	Alcohol dehydrogenase	PQQ/heme C/3 heme C's	Membrane-bound	α/β/small	*Gluconobacter* sp.	21
					Acetobacter sp.	21

(*Continued on next page*)

Table 1 Continued

	Prosthetic group	Location	Component	Organism	Ref.
Glucose dehydrogenases					
Glucose dehydrogenase (m)	PQQ	Membrane-bound	Monomeric	Enterio bacteria	12
				Gluconobacter sp.	12
				Pseudomonas sp.	12
				Acinetobacter calcoaceticus	12
				Acetobacter sp.	12
Glucose dehydrogenase (s)	PQQ	Periplasm	Homodimeric	*Pseudomonas* sp. N11	22
				Acinetobacter sp.	12
Cyclic alcohol dehydrogenase	PQQ	Membrane-bound	Monomeric	*G. frateurii* CHM9	23
D-Arabitol dehydrogenase	PQQ	Membrane-bound	Heterodimeric ($\alpha\beta$)	*G. suboxydans* IFO3257	24
Formaldehyde dehydrogenase	PQQ	Membrane-bound	Homotetrameric	*Methylococcus capsulatus*	25

Lupanine hydroxylase	PQQ/heme C	Periplasm	Monomeric	*P. putida*	26
Sorbitol dehydrogenase	PQQ/heme C/3 heme C's	Membrane-bound	α/β/small	*Gluconobacter* sp.	27
		Membrane-bound	Oligomer?	*G. suboxydans* IFO3255	
Sorbose/sorbosone dehydrogenase	PQQ	Periplasm	Heterodimeric	The strain DSM4025	28
Quinate dehydrogenase	PQQ	Particle-bound	Monomeric	*A. calcoaceticus*	16
				Gluconobacter sp.	
1-Butanol dehydrogenase	PQQ	Periplasm	Monomeric	*P. butanovora*	29
	PQQ/heme C	Periplasm	Monomeric	*P. butanovora*	30
Glycerol dehydrogenase	PQQ	Membrane-bound	Monomeric	*G. industrius*	31

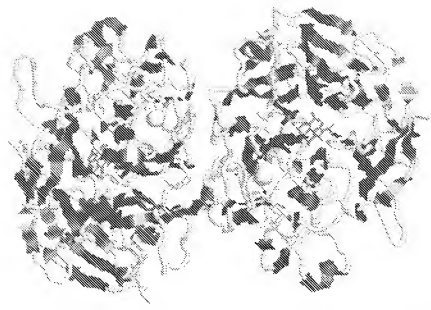

Figure 2 Overall structure of water-soluble quinoprotein glucose dehydrogenase (PQQGDH-B). This model was complemented by the addition of PQQ, Ca^{2+}, some loop regions, and the energy minimization based on previously reported model (From Ref. 68) (PDB code: 1QBI).

PQQ-dependent glucose dehydrogenases (PQQGDHs) have also been studied extensively. PQQGDHs are described in the next section.

1.2 PQQ Glucose Dehydrogenases—The Basic Science and Industrial Application

There are two types of glucose dehydrogenases harboring PQQ as their prosthetic group (44,45). Membrane-bound type glucose dehydrogenase (PQQGDH-A) has been isolated from various Gram-negative bacteria such as *Escherichia coli*, *Acinetobacter calcoaceticus*, *Pseudomonas* sp., and acetic acid bacteria (12). PQQGDH-As are all single peptide with MWs of about 87 kDa containing one PQQ molecule (46,47). PQQGDH-As make a bioenergetic contribution via coupling of the oxidation of glucose to the respiratory chain through ubiquinone (48,49). The five genes encoding PQQGDH-A have been elucidated (46,47,50–52). The 3-D structure of PQQGDH-A is predicted to be a β-propeller composed of eight W-motifs, based on the homology modeling with PQQMDH (53) and also based on the CD spectroscopy of an enzyme from which the membrane spanning region was deleted (54). The N-terminal region was predicted to be the membrane spanning the anchoring region (55). The authors have reported the first site-directed

mutagenesis study on a PQQ enzyme, PQQGDH-A. Since then, several mutations were introduced in this enzyme, including the studies introduced in this review, to elucidate the enzyme mechanisms (56–66).

Besides the membrane-bound glucose dehydrogenase, *A. calcoaceticus* possesses a completely different PQQGDH, the water-soluble glucose dehydrogenase (PQQGDH-B or s-GDH), which does not share any obvious homology with the primary structures of other PQQ enzymes (67). The BLAST search for PQQGDH-B homology identified two open reading frames from the *E. coli* K-12 strain MG1655 genome and *Synechocystis* sp. strain PCC6803 genome and two incomplete sequences from the genomes of *Pseudomonas aeruginosa* and *Bordetella pertussis*. The functions of these four deduced open reading frames are uncertain, and the predicted protein localization also differs using the prediction program (PSORT and Signal P) (68,69).

PQQGDH-B is a homodimeric enzyme consisting of an identical subunit of approximately 50 kDa (67,70). The monomer has one PQQ molecule and three Ca^{2+} ions, two of which are located in the dimer interface and the third Ca^{2+} ion is near PQQ (68). The physiological roles of PQQGDH-B have not yet been elucidated. PQQGDH-B does not couple with the respiration chain of *A. calcoaceticus*. The substrate specificity profile of PQQGDH-B is broad compared with that of PQQGDH-A. This enzyme catalyzes the oxidation of glucose, allose, 3-*O*-methyl-glucose, and also the disaccharide lactose, cellobiose, and maltose (71). PQQGDH-B contains a 24-amino acid signal peptide at its N-terminus and secreted in the periplasmic space after excision of the signal sequence. PQQGDH-B is also a β-propeller, but apparently forms a 6-bladed structure (68). PQQ resides in a deep, broad, positively charged cleft at the top of the propeller near the 6-fold pseudo-symmetry axis (72). In this model, PQQ is directly exposed to the solvent. Ca^{2+} ion is bound to N6, O7A, and O5 atoms of PQQ. These bonds are similar to that of PQQMDH, and it indicates that catalysis of Ca^{2+} ion near the PQQ requires a cofactor. The active site of PQQGDH-B is composed of loop1D2A, loop2D3A, loop4BC, loop4D5A, and loop6BC. The substrate biding residues have been reported and are included mainly in loop1D2A, loop2D3A, and loop4BC (72). Among them, His168 was specified as an important residue that works for proton abstraction from substrate because His168 is the only base close to the glucose O1 atom, and glucose C1 atom is positioned directly above the $PQQH_2$ C5 atom (72).

1.3 The Industrial Significance of PQQGDH: The Glucose Sensors

Diabetes mellitus is a serious metabolic disorder that places patients at increased risk of coronary and vascular disease, as well as debilitating

conditions such as retinopathy, nephropathy, and neuropathy. Therefore rapid and accurate blood glucose monitoring is essential for treating critically ill patients and managing diabetic patients.

The glucose sensor is a traditional biosensor and was first reported by Clark in 1962 (73). Clark's sensor was based on glucose oxidase (GOD) as its sensor constituent, and GOD-based glucose sensors dominate the current market. GOD is categorized as a stable protein and may be easily produced and purified from *Aspergillus* sp. GOD is an electron mediator-type glucose sensor. The inherent property of GOD is that it utilizes oxygen as the electron acceptor. This limits the further application in this field because enzyme activity is a function of oxygen partial pressure (74–76). Various glucose sensors employing PQQGDHs have been reported (77–81).

The merits of using the PQQGDHs as a glucose sensor component are as follows:

1. PQQGDHs show high catalytic efficiency compared with GOD. The high activity allows rapid glucose sensing.
2. PQQ is tightly bound to GDH; therefore it is not necessary to add an extra cofactor like NAD (P).
3. PQQGDHs do not utilize dissolved oxygen as its electron acceptor during glucose oxidation. This property enhances accurate measurement of glucose in the human blood.

Focusing these merits, PQQGDH-B glucose sensors are already on the market. However, despite their superior features, further improvements are required. This is particularly true when PQQGDH is compared with GOD, which has better substrate specificity and operational stability. The establishment of economical recombinant enzyme production system is also essential.

The authors' research group initiated and is currently the only group engaged in the protein engineering of PQQGDHs to develop an optimized glucose sensor enzyme. This review summarizes the current status of PQQGDH protein engineering.

2 PROTEIN ENGINEERING OF PQQGDH-A

AQ1

Highly homologous primary structures have been observed in PQQGDH-As, which have been cloned from various Gram-negative bacteria; however, the enzymatic characteristics are dependent upon the derived bacterial sources. Although their tertiary structure was hard to elucidate due to hydrophobic properties, the highly homologous primary structure of this protein enabled us to initiate the protein engineering of this enzyme based on the homologous recombination to construct a chimeric enzyme library (58,60,63).

Among various properties, we focused on the difference in the cofactor binding stability as the marker for the chimeric enzyme library. PQQGDHs require divalent ion for holoenzyme formation with PQQ; however, divalent ions such as Ca^{2+} are removed by the presence of chelating reagents such as EDTA, resulting in apoenzyme formation (82). Therefore EDTA tolerance can be interpreted as an indicator of cofactor binding stability. *A. calcoaceticus* PQQGDH-A is a representative EDTA-tolerant enzyme, whereas *E. coli* PQQGDH-A is a representative EDTA-sensitive enzyme (57,58,70). The highly homologous primary structure between *E. coli* and *A. calcoaceticus* PQQGDH-A structural genes provided a strategy for the construction of a chimeric enzyme library based on homologous recombination. The investigation of the chimeric PQQGDH-A library resulted in the elucidation of the region responsible for EDTA tolerance (58,60) (Table 2). T2

One of the chimeric enzymes (designated as E97A3) showed the increase in the thermal stability of which the N-terminal 97% region is from *E. coli* and the remaining 3% is from *A. calcoaceticus* PQQGDH-A (57). This observation suggested that the interaction between C-terminal and N-terminal regions may play a crucial role in maintaining the overall structure of β-propeller proteins (63).

We have also carried out the first site-directed mutagenesis studies on PQQ enzymes, particularly PQQGDH-A, focusing on the C-terminal highly conserved region, previously postulated as the putative PQQ binding site (83). Cleton-Jansen et al. (50) reported an altered substrate specificity of a mutant PQQGDH-A in *Gluconobacter oxydans*, for which substrate specificity was enlarged by the substitution of the conserved C-terminal His region. Based on this information, site-directed mutagenesis studies on the conserved C-terminal His residues of *E. coli* PQQGDH-A (His775) and of *A. calcoaceticus* (His781) were carried out (59,62). The substitution of *E. coli* His775 to Asn showed the increase in both Km value (from 0.9 to 1.5 mM) and Vmax/Km ratio (from 116 to 287 U/mg protein mM) for glucose compared with wild type (Table 2). The substrate specificity of His775Asn drastically changed and increased vs. wild-type *E. coli* PQQGDH-A. The Vmax/Km ratios for all substrates except for glucose decreased as compared with wild type; consequently, His775Asn scarcely oxidized sugars other than glucose. His775Asp also showed a significant increase in Km values for all the saccharides used in the study (Table 2), and showed improvement of the substrate specificity compared with wild-type *E. coli* PQQGDH-A, as did His775Asn. Amino acid substitution at His781 in *A. calcoaceticus* also significantly affected substrate specificity.

On the basis of the accumulated information from these studies, we constructed an enzyme composed of all the regions that showed improved

Table 2 Substrate Specificity Profiles of PQQGDH-A His775 Variants

	Wild type	His775Asn	His775Asp	His775Glu	His775Lys	His775Ser	His775Leu	His775Tyr	His775Trp
Activity (U/mg)	110	417	140	79	5.6	195	7.9	3.1	1.1
D-Glucose	100	100	100	100	100	100	100	100	100
2-Deoxy-glyucose	81	30	52	47	177	64	39	46	49
D-Mannose	30	1	0	3	0	3	1	2	2
D-Allose	105	13	21	29	161	73	29	105	58
D-Galactose	38	2	0	6	6	7	6	12	3
D-Xylose	48	4	1	4	16	5	4	3	9
Maltose	14	5	3	2	23	4	2	1	4

Substrate concentration is 1 mM.
The values were the relative activity compared with the activity toward glucose as the substrate.

Table 3 The Enzymatic Properties of Multichimeric PQQ Glucose Dehydrogenases

	E.coli PQQGDH	H775N		E97A3		E97A3 H775N		E32A27E41		E32A27 E38A3		E32A27E41 H782N		E32A27E38A3 H782N	
			+		+		+		+		+		+		+
EDTA tolerance	–	–		–		–		+		+		+		+	
T1/2 at 45°C	< 1	< 1		< 1		1.4		27		21		7.7		39	
D-Glucose	100(%)	100(%)		100(%)		100(%)		100(%)		100(%)		100(%)		100(%)	
2-Deoxy-D-glucose	69	11		76		27		69		61		31		18	
D-Mannose	5	0		4		0		7		11		13		1	
D-Allose	81	4		93		29		92		87		58		46	
D-Galactose	8	0		7		0		18		17		15		7	
D-Xylose	21	2		10		0		37		35		17		1	
Maltose	3	2		0		0		4		6		13		7	

Substrate concentration is 1 mM. The values were the relative activity compared with the activity toward glucose as the substrate. ◆: His775 or His782 mutation; +: shows EDTA tolerance; –: does not show EDTA tolerance.

enzymatic characteristics with the goal of engineering an optimized sensor enzyme.

Multichimeric PQQGDH-As with improved enzymatic characteristics were engineered by substituting and combining various PQQGDH-A constructs: the region responsible for EDTA tolerance (A27 region), for the thermal stability (A3 region), and for the substrate specificity (conserved His residue in PQQGDH-A) (57,63). The resulting chimeric PQQGDH-As were E32A27E38A3 His782Asn and E32A27E38A3 His782Asp. Both multichimeric PQQGDH-As showed increased cofactor binding stability, thermal stability, and alteration in substrate specificity. Moreover, E32A27E38A3 His782Asp showed a 10-fold increase in the Km value for glucose compared with the wild-type *E. coli* PQQGDH-A (Table 3). T3

This study indicated the complementarity of the protein regions responsible for the improvement of different enzymatic properties of PQQGDH-A.

3 PROTEIN ENGINEERING OF PQQGDH-B AQ1

3.1 3-D Engineering Approaches

We have carried out the protein engineering on PQQGDH-B for the improvement of thermal stability, catalytic efficiency, and enhanced substrate specificity. Although the tertiary and quaternary structures of this enzyme are now available, these only provide limited information on enzyme function. Successful engineering will still require multiple strategies; our approach uses a combination of random mutagenesis and rational design of amino acid substitutions. We have been attempting to develop an optimized PQQGDH-B for sensor applications. In this section, we summarize our current efforts to engineer PQQGDH-B.

3.1.1 Glu277Lys

Prior to the elucidation of the tertiary structure of PQQGDH-B, the authors carried out the site-directed mutagenesis on PQQGDH-B, the putative active site based on the enzymatic properties of PCR mutants of this enzyme (71). The random mutant enzyme found in our laboratory, designated as No.87, contained eight amino acid substitutions. This mutant showed a decreased Km value and also a decreased EDTA tolerance, indicating decreased holoenzyme and thermal stability compared with the wild type. On the basis of mutational analyses, we found that the substitution of Glu277 residue with Gly was responsible for the properties of No.87. Moreover, mutational analyses on the neighboring amino acid residues of Glu277, Asp275Glu, Asp276Glu, Ile278Phe, and Asn279His were also carried out. Considering

that Asp275Glu, Asp276Glu, and Glu277Gly showed drastic decreases in EDTA tolerance, we assumed that this region might be the PQQGDH-B active site and/or a binding site for Ca^{2+} or PQQ. This was later confirmed by elucidation of the tertiary structure. Glu277 variants all showed decreased Km values and altered substrate specificity profiles. Among them, Glu277Lys showed similar enzymatic activity and thermal stability to the wild-type enzyme, but its catalytic efficiency (kcat/Km) was approximately 3-folds higher compared to the wild type (349 to 128 s^{-1} mM^{-1}) (Table 4). According to the 3-D structure of PQQGDH-B, the position of Glu277 is located at strand 4C. This strand is connected to loop4BC, one of the loop regions that creates the enzyme's cavity. Glu277 mainly interacts with Ca^{2+} ion (II) that is located in the dimer interface loop region. Therefore the replacement of Glu277 with other amino acids may affect its dimer conformation. Furthermore, the neighboring amino acid residue, Asp275, apparently works as one of the donated residues connecting a water molecule to Ca^{2+} ion (III). Asp276 is included in Ca^{2+} ion binding site (I) that is located at an active site. In addition, Asn279 also contributes in connecting a water molecule to Ca^{2+} ion (III). Thus the region from Asp275 to Asn279 is the hot spot related to all Ca^{2+} ion binding site and an active site in PQQGDH-B. We can conclude that the decreased EDTA tolerance and thermal stability are consistent with the location and function of these residues.

The recent emergence of self-testing markets for blood glucose requires less painful methods for taking the sample and for enhanced measurement,

Table 4 Kinetic Parameters of Wild-Type and Glu277Lys PQQGDH-B for Various Substrates

	Wild type			Glu227Lys		
	Km (mM)	kcat (s^{-1})	kcat/Km (s^{-1} mM^{-1})	Km (mM)	kcat (s^{-1})	kcat/Km (s^{-1} mM^{-1})
Glucose	26.8	3436	128 (100%)	8.8	3071	349 (100%)
2-Deoxy-glucose	90	331	4 (3%)	88	1063	12 (3%)
Mannose	22	267	12 (9%)	22	861	39 (11%)
Allose	35.5	2509	71 (55%)	21	4563	287 (82%)
3-*O*-methyl-glucose	28.7	3011	105 (82%)	27	3198	118 (34%)
Galactose	5.3	232	44 (34%)	6.8	630	78 (22%)
Xylose	14.3	201	14 (11%)	34	678	20 (6%)
Lactose	18.9	1659	88 (69%)	7.5	1795	239 (68%)
Maltose	26	1930	74 (58%)	14.3	1015	71 (20)%

simplicity, and reliability. Semi- or minimally invasive systems are considered optimal. Minimization of the blood or interstitial fluid (ISF) sample implies the need for high catalytic efficiency in the sensor element. As Glu277Lys showed three times higher catalytic efficiency, this variant has great potential as a component of a highly sensitive glucose monitoring system.

3.1.2 Ser231Lys

Another PCR mutant of PQQGDH-B, Ser231Cys, was found to retain higher thermal stability than the wild-type PQQGDH-B (69) (Fig. 3). Therefore the F3 authors replaced Ser231 with a series of amino acids and analyzed their impact on thermal stability. Ser231Lys showed the highest thermal stability at 55°C without decreasing catalytic activity. Ser231Lys showed more than an 8-fold increase in its half-life (Ser231Lys: 40 min, wild type: 5 min) during the thermal inactivation at 55°C compared with the wild-type enzyme without a decrease in catalytic activity. Therefore higher yield in active enzyme preparation is expected, which may improve the cost effectiveness of glucose sensor component production using this enzyme. Moreover, higher thermal stability usually results in higher storage stability; therefore the application of this mutant enzyme as a glucose sensor constituent may develop into a stable glucose sensor construction.

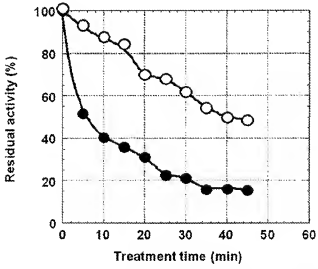

Figure 3 Thermal stability of wild-type and Ser231Lys PQQGDH-B at 55°C. ○: Ser231Lys; ●: wild type. The residual activity of PQQGDHs was determined at 25°C.

The replacement of Ser231 with hydrophobic residues does not affect its thermal stability and substrate specificity profile. Furthermore, it is reasonable to suggest that the charge or the size of the side chain at the 231st positioned residue will not show any correlation with its enzymatic properties. Generally, β-propeller fold can be divided into three regions: (1) β-sheet regions that provide scaffold structure; (2) loopBC and loopDA regions (loop regions connecting strand B and strand C, and then strand D and strand A, respectively; these tend to be the functional regions, coenzyme or metal ion binding); and (3) loopAB and loopCD regions, which are located opposite the functional regions. Since Ser231 is located in loop3CD, the replacement of this residue might not affect the catalytic properties of this enzyme.

Modeling analysis of Ser231Lys suggested that the replacement of Ser231 with Lys effectively increased the hydrophobicity in the loop3CD region. This observation suggested that the increase in hydrophobic interaction strengthened the packing of W-motif and/or β-propeller structure.

3.1.3 Asn452Thr

The conserved C-terminus amino acid residues in PQQGDH-A, His775 (in *E. coli* PQQGDH), and His781 (in *A. calcoaceticus* PQQGDH-A) were shown to be responsible for their substrate specificity profiles (59,62). The primary structure of PQQGDH-B has little similarity to that of PQQGDH-As. However, in both enzymes, the orientation of the active site is in the opposite site of the region where the C-terminus and N-terminus interact to circularize the β-propeller. On the basis of this similarity, we assumed that residues with the same 3-D orientation could affect the substrate specificity of both PQQGDH-A and PQQGDH-B. This would make the C-terminus the region of interest. Moreover, according to the structural information on the PQQGDH-B active site, substrate glucose locates in the cavity composed of 1D2A, 2D3A, 3BC, 4D5A, and 6BC loops and interacts with the amino acid residues located at 1D2A, 2D3A, and 3BC (72). However, loop6BC does not have amino acid residues that interact with glucose. One of the characteristic properties of GDH-B substrate specificity is that PQQGDH-B reacts with disaccharide such as lactose and maltose. If loop6BC is not involved in substrate binding, the engineering of loop6BC for direct substrate interaction or interaction with other loops to create indirect substrate interaction may alter the size of the cavity and create novel catalytic properties. More specifically, such engineering could result in PQQGDH-B with narrowed substrate specificity. Therefore we have introduced amino acid substitutions into the loop6BC region to improve the substrate specificity profile. We focused on polar amino acid residues in loop6BC region and constructed a series of variants. Among these mutants, we found that Asn452Thr did, in

fact, show a narrowed substrate specificity profile without a decrease in the catalytic activity (84).

Because Asn452Thr showed greater substrate specificity than the wild-type enzyme, we investigated the effect of the presence of lactose on the glucose measurement using both wild-type PQQGDH-B and Asn452Thr (Fig. 4). When using the wild-type enzyme, with increased lactose concentration, discoloring reaction of DCIP toward 10 mM glucose increased. No saturation was observed up to 25 mM lactose. In the presence of 10 mM lactose, the effect was more than 10%. This influence was due to the high affinity toward lactose and also catalytic efficiency compared with those for glucose. In contrast, when using Asn452Thr to measure glucose, the addition of 25 mM lactose only caused a 5% increase in the apparent rate of the reaction. Furthermore, saturation is reached at around 15 mM lactose concentration, and the signal can be increased by a maximum of 5%. This was due to the lower affinity for lactose and higher affinity for glucose compared with the wild-type enzyme. Considering that Asn452Thr showed lower Vmax/Km values toward maltose and galactose than the wild-type enzyme, the engineered enzyme appears to have glucose specificity.

F4

3.2 4-D Engineering Approaches

Optimized sensor fabrication using PQQGDH-B requires maximization of enzyme stability. There are several ways to increase the protein thermal

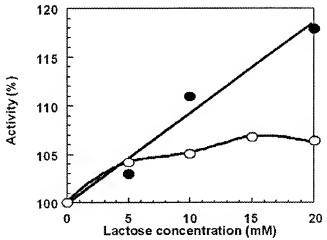

Figure 4 The reactivity of wild-type and Asn452Thr PQQGDH-B toward 10 mM glucose in the presence of lactose. O: Asn452Thr; ●: wild type. The rate of reaction toward 10 mM glucose, in the absence of lactose, is presented as 100%.

stability, such as increasing the interaction of amino acid residues responsible for conformational stability using site-directed mutagenesis. It has also been proposed that by excluding conformers that are in the denaturation pathway, the stability of protein may be enhanced. On the basis of the assumption that the first step of the inactivation of PQQGDH-B is dimer dissociation, the stabilization of quaternary structure should enhance the stability of PQQGDH-B.

In order to prevent the dissociation of quaternary structure, we designed chemically cross-linked PQQGDH using glutaraldehyde (81). Chemically linked PQQGDH-B showed higher thermal stability than wild-type enzyme; the half-life at 55°C is 63 min whereas that of native enzyme is 4 min. This suggested that the thermal stability of PQQGDH-B is significantly improved by stabilizing quaternary structure. However, chemical modification resulted in a decrease in specific activity (less than 10% of native enzyme) as a result of nonspecific modification of amino acid residues. Therefore additional rational design parameters must be applied.

Here we present our efforts in stabilizing PQQGDH quaternary structures by protein engineering (Table 5). T5

3.2.1 Tethered PQQGDH-B

In order to decrease the chance of dissociation of PQQGDH-B subunits, we have attempted to construct a linked dimeric PQQGDH-B by the in-frame gene fusion technique (85). A tethered PQQGDH-B is constructed using the linker peptide, "Glu-Leu-Gly-Thr-Arg-Gly-Ser-Ser-Arg-Val-Asp-Leu-Gln," derived from a part of β-galactosidase in expression vector pTrc99A. We produce a tethered PQQGDH-B in *E. coli* as the active soluble enzyme (86). This enzyme shows enhanced thermal stability over the native enzyme expressed in *E. coli*. At incubation temperatures above 45°C, the residual

Table 5 Comparison of the Enzymatic Properties of Engineered PQQGDH-Bs

	Half-life time at 55°C (min)	Specific activity (U/mg protein)	Km (mM)
Wild type	5	4104	25
Ser231Lys	40	3313	27
Cross-linking	63[a]	389	20
Tethered	16	897	20
Ser415Cys	183	4134	16

[a] Mixture of cross-linking status.

activity of a tethered PQQGDH-B is more than twice that of the native dimeric enzyme. Moreover, we evaluate the thermal stability at 55°C using half-life time. A tethered PQQGDH-B shows longer half-life time at 55°C (17 min) compared with the wild type (5 min) (Fig. 5). The Vmax value of tethered PQQGDH-B is 897 U/mg protein with about 10–40% of the catalytic activity of the native one. The presence of the linker region prohibits the complete dissociation of the subunits. By linking the subunits, the entropy of denaturation decreased with a concomitant increase in the thermal stability. However, the length and flexibility of linker peptide should be further optimized to construct a thermostable tethered enzyme with appropriate catalytic activity. F5

3.2.2 Ser415Cys

Although the stabilization of the quaternary structure of PQQGDH-B by the chemical modification (81) or tethering with linker peptide (86) improves the thermal stability of PQQGDH-B, these modifications resulted in a decrease in catalytic activity. We therefore attempted to introduce disulfide bond into the dimer interface of PQQGDH-B to form covalent bonds between subunits and to stabilize its quaternary structure (87). We searched the residues, which are not associated with the active site but face each other. We specified Ser415; this residue is in loop5CD, does not participate in the active site, and faces the dimer interface. The distance between each side chain is 6.12 Å (Oγ–Oγ), so

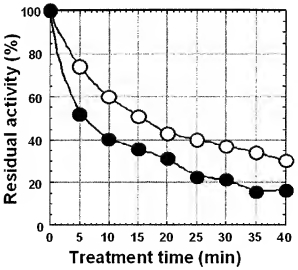

Figure 5 Thermal stability of wild-type and tethered PQQGDH-B at 55°C. ○: Tethered PQQGDH-B; ●: wild type. The residual activity of PQQGDHs was determined at 25°C.

that a disulfide bond may be formed after the substitution of a Cys residue. Ser415 is therefore selected for substitutions to Cys. Ser415Cys shows 36 times higher thermal stability at 55°C than wild type (half-life; 183 vs. 5 min) without any decrease in catalytic activity (kcat; 3461 s^{-1}) (Fig. 6). Moreover, **F6** after incubation at 70°C for 10 min, Ser415Cys retains more than 90% of GDH activity. Disulfide bond formation between the subunits is confirmed by comparing SDS-PAGE in the presence or absence of reductants. Our results indicate that the introduction of one Cys residue in each monomer of PQQGDH-B resulted in the formation of a disulfide bond at the dimer interface and thus achieving a large increase in the thermal stability of the enzyme. Ser415Cys shows about four times higher thermal stability compared with Ser231Lys at 55°C.

3.3 Recombinant Production of PQQGDH

Considering the huge market for self-monitoring blood glucose sensors, and the potential to engineer these enzymes, the next obvious challenge is to produce recombinant enzymes efficiently in recombinant systems.

The expression of each recombinant PQQGDH-A and PQQGDH-B of *A. calcoaceticus* or PQQGDH-A of *E. coli* using *E. coli* as the host strain was first reported by Cleton-Jansen et al. (67). Since both enzymes require PQQ and bivalent metal ion for enzymatic activity, recombinant PQQGDHs in *E.*

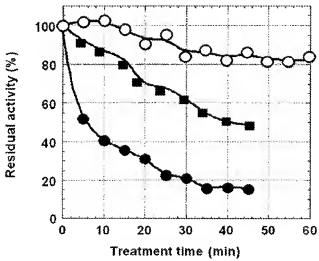

Figure 6 Thermal stability of Ser415Cys PQQGDH-B compared with wild-type and Ser231Lys at 55°C. ○: Ser415Cys; ●: wild type; ■: Ser231Lys. The residual activity of PQQGDHs was determined at 25°C.

coli were produced as apoenzymes. We found that the apo-PQQGDHs are less thermally stable than holo-PQQGDHs. In order to prevent the denaturation of recombinant PQQGDHs during *E. coli*-based production, we first tried recombinant PQQGDH-A production with PQQ in the medium (88). The presence of PQQ and Ca^{2+} in the medium resulted in increase productivity. It is known that PQQ is synthesized in several microorganisms, including *Acinetobacter*, *Pseudomonas*, and *Klebsiella*, and the operon-encoding PQQ biosynthetic pathway has been cloned from several genera. The introduction of the PQQ biosynthesis operon from *E. coli* enabled the PQQ biosynthesis. An *E. coli* strain carrying both a vector with the *Klebsiella*-derived PQQ biosynthesis operon (89) and an expression vector for the PQQGDH-A structural gene was generated. This double recombinant produced holo-PQQGDH-A. However, this system had the problem that the population of *E. coli* cells harboring both plasmids decreased during cultivation.

Considering the genetic instability, the integration of the PQQ operon into the host chromosome may be preferable. Alternatively, a PQQ-synthesizing bacterium could be used as the expression system of PQQGDH in such microorganisms which was also reported in *Acinetobacter* strains and *Pseudomonas* strains. However, the use of the broad host range vectors in these host strains has inherent problems with respect to the production of recombinant proteins.

However, *Klebsiella* can synthesize PQQ and also maintain several *E. coli* expression vector systems. We recently reported recombinant PQQGDH-B production utilizing *Klebsiella pneumoniae* as the host strain and a conventional *E. coli* expression vector for PQQGDH-B production (90). The recombinant *K. pneumoniae* expressed PQQGDH-B in its holoform at levels about equal to that achieved in recombinant *E. coli* (Fig. 7). The signal sequence of recombinant PQQGDH-B was correctly processed. F7

In the above-mentioned recombinant systems, PQQGDHs are being accumulated in the cell during production. Therefore cell disruption is essential for the recovery of holoenzyme. Considering that PQQGDH-B is secreted in the periplasmic space of the Gram-negative bacteria by posttranslationally processing the signal peptide, extracellular production of recombinant PQQGDH-B will be expected. We have achieved this type of production of PQQGDH-B using the methylotrophic yeast *Pichia pastoris*. *P. pastoris* is known for the expression of heterologous genes requiring secretion. One of the important factors for this system is the alcohol oxidase I (AOX1) promoter of *P. pastoris* which can regulate the expression of foreign genes by the concentration of methanol. Furthermore, since the molecular genetic manipulation of *P. pastoris* is similar to that of the well-characterized *Saccharomyces cerevisiae* expression system, *P. pastoris* is also widely accep-

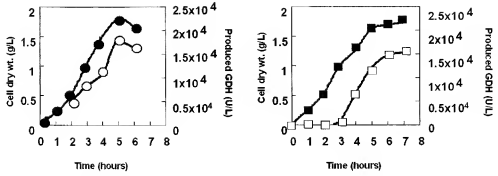

Figure 7 Time course of PQQGDH-B production in *E. coli* PP2418 and *K. pneumoniae* NCTC418. ●: Growth of *K. pneumoniae*; ○: productivity in *K. pneumoniae*; ■: growth of *E. coli*; □: productivity in *E. coli*. Each culture contains 1 mM $CaCl_2$.

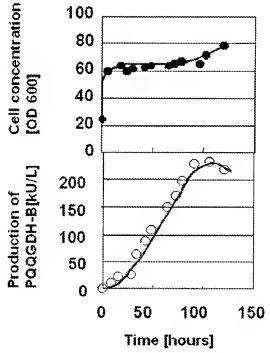

Figure 8 Growth curve and GDH production in recombinant *P. pastoris*. ●: Cell concentration OD600; ○: produced PQQGDH-B (kU/L).

ted. Instead of the native signal sequence of PQQGDH-B, the *S. cerevisiae* α-factor signal sequence was used for the secretion of PQQGDH-B in *P. pastoris* (91). The productivity of secreted PQQGDH-B reached 218 kU/l (43 mg/l) which was almost the same as that of the recombinant PQQGDH-B previously produced in *E. coli* (Fig. 8). The secreted PQQGDH-B in *P. pastoris* F8 was glycosylated but showed similar enzymatic properties as compared with those of the recombinant PQQGDH-B produced in *E. coli*. Further optimization of the downstream process and culture condition for high-level production of the recombinant PQQGDH-B by *P. pastoris* is expected to achieve industrial level production.

4 APPLICATION OF ENGINEERED PQQGDH FOR GLUCOSE SENSORS AND FOR DNA SENSORS

4.1 Glucose Sensors

Ultimate goal in the engineering of PQQGDHs is the construction of an optimized enzyme for monitoring glucose.

Our first attempt involved the utilization of engineered PQQGDH-A for the construction of a glucose sensor with extended dynamic range (92). Fig. 9 shows the correlation between glucose concentration and enzymatic F9 activities of both wild-type *E. coli* PQQGDH-A and His775Asp. The enzymatic activity of wild-type *E. coli* PQQGDH-A almost saturated at the glucose concentration higher than 10 mM. The enzymatic activity of His775Asp increased with the increased glucose concentration between 10

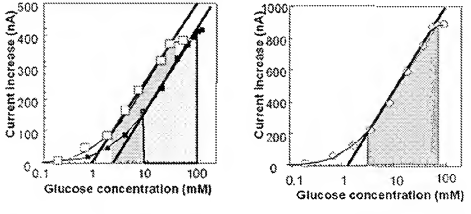

Figure 9 A calibration curve of all the ranger glucose sensor, employing engineered PQQGDHs, His775Asn and His775Asp. □: His775Asn (linearity; 2–31 mM); ■: His775Asp (linearity; 9–80 mM); O: His775Asn and His775Asp (linearity; 3–70 mM).

and 50 mM. With diabetes, glucose concentration in blood is often over 200 mg/dl (11.1 mM). Considering that in disposable glucose sensors blood samples are directly subjected to the sensor element, the high Km value of His775Asp is an important property of the sensor element. The increased dynamic range of glucose measurement with the engineered enzyme enabled us to develop a strategy for a glucose sensor with an expanded dynamic range (92). The proposed strategy improves the dynamic range of the biosensor by utilizing protein-engineered PQQGDH-As with different Km values, which, in turn, expands the dynamic range.

The composite extended-range glucose sensor employing two engineered PQQGDH-As, His775Asp and His775Asn, was demonstrated. The extended-range glucose sensor showed not only an expanded dynamic range (3–70 mM), but also greater substrate specificity for glucose due to the engineered enzymes (Fig. 9).

Another type of glucose sensor was constructed utilizing one of the multichimeric PQQGDH-As, E32A27E38A3 His782Asp, with increased cofactor binding stability, thermal stability, an alteration in substrate specificity, and increased Km value for glucose compared with the wild-type *E. coli* PQQGDH-A (93). The application of E32A27E38A3 His782Asp in amperometric glucose sensor construction achieved an expanded dynamic range together with increased operational stability and greater substrate specificity. The glucose sensor can measure glucose from 5 to 40 mM, which should allow for the direct measurement of high blood glucose levels in diabetic patients.

We have also reported a glucose enzyme sensor with engineered PQQGDH-B. We employed the enzyme with increased thermal stability, Ser231Lys (81). The residual activity after heat treatment at 60°C for 2 h was 80% of the initial activity, whereas the electrode fabricated with wild-type PQQGDH-B was 30% (Fig. 10). This result showed that the sensor employing Ser231Lys exhibited significantly enhanced thermal stability and promises a high operational stability. F10

4.2 Application of PQQGDH for DNA Sensors

DNA sensing has become very important since it is a powerful tool for detection of the toxic microorganisms in food (or the environment) and may also be used for fundamental studies in molecular biology (94). Many types of DNA sensing systems have been developed such as DNA microarrays based on fluorescence detection of the hybridization using the probe DNA labeled with fluorescent compounds. An electrochemical DNA sensing system would also be of interest since it only requires an electrode and relatively simple electrochemical instrumentation. Most current electrochemical DNA sensing

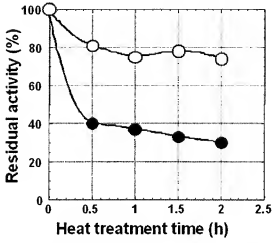

Figure 10 Thermal stability of the sensor employing PQQGDH-Bs at 60°C. ○: Ser231Lys; ●: wild type. After heat treatment, the responses at 0.99 mM glucose were measured at 25°C. The measurement was carried out in 10 mM MOPS-NaOH (pH 7.0) containing 1 mM methoxy-PMS, 1 μM PQQ, and 1 mM $CaCl_2$. The operating potential: +100 mV vs. Ag/AgCl; temperature for measurement: 25°C.

systems are based on electrochemically active probes that detect the hybridization events. Examples include the use of redox intercalators to recognize the double-stranded DNA, DNA detection via a DNA-mediated electron transfer to the electrode using mediators, and the use of ferrocene-labeled oligonucleotide probe which is hybridized to the DNA immobilized on the electrode. To improve the sensitivity, an enzyme label was used for the detection of hybridization since enzyme labels can dramatically amplify the signal produced by DNA hybridization. We proposed a novel DNA sensing system utilizing PQQGDH-B as the probing enzyme for DNA detection.

In order to detect the hybridization of the DNA probe with the target DNA, the PQQGDH was chemically conjugated with avidin. Using the sensor system, we aimed to detect the specific DNA sequence of a pathogenic bacteria, *Salmonella* virulence (*invA*) gene. The probe DNA bearing complementary to the specific sequence of *invA* gene was immobilized onto the carbon paste electrode, and the biotinylated target DNA was hybridized to it. After the hybridization, PQQGDH–avidin conjugate was added, and the electric current generated from glucose oxidization catalyzed by PQQGDH via 1-methoxyphenazine methosulfate (m-PMS) as a mediator was measured. The sensor response was increased by glucose addition, and it increased in the range from 5.0×10^{-8} to 1.0×10^{-5} M as DNA concentration increased in the presence of 6.3 mM glucose (Fig. 11). F11

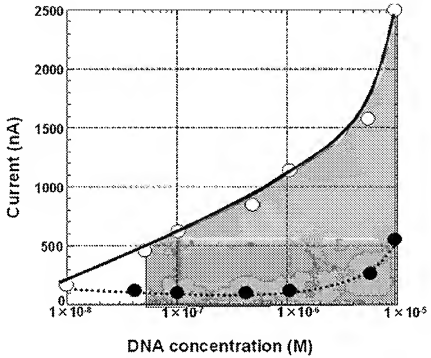

Figure 11 Calibration curve of the sensor employing PQQGDH-B for DNA. The gray colored region displayed the measurable concentration in this study. For measurement, 0.2 unit of the PQQGDH-avidin conjugate was added to 10 ml of 10 mM MOPS-NaOH (pH 7.0) containing 1 mM m-PMS, 1 mM $CaCl_2$, 1 μM PQQ, and 6.3 mM glucose. The operational potential: +100 mV vs. Ag/AgCl. Temperature for measurement: 25°C. O: Probe DNA; ●: control DNA.

Routine use of DNA-based analyses, such as SNP or pathogen detection, will require both simplicity and sensitivity in sensor design. Our DNA sensing system has the advantage of stability of substrate compared to the peroxidase since the hydrogen peroxide is very reactive and decreases quickly. Glucose oxidase (GOD) may also be used, but the samples for DNA sensing can be from sources such as human blood, foods, and soils so that the dissolved oxygen concentration (a variable in the GOD reaction) might differ.

5 CONCLUSION

Due to the high specific activity of PQQGDH-B vs. PQQGDH-A, current glucose sensor technology employing GDH is limited to PQQGDH-B.

However, comparing the catalytic efficiencies (kcat/Km) of both PQQGDH-A and PQQGDH-B, no significant difference is observed. Considering the narrow substrate specificity of PQQGDH-A, the development of enzyme sensor employing this enzyme will expand the use of quinoprotein dehydrogenases. The applications of GOD may be limited due to its low catalytic efficiency (compared with both types of PQQGDH) and its dependence on O_2 partial pressure. Our recent advances in the protein engineering of PQQGDHs indicate that these enzymes may be the most versatile and ideal for glucose sensors. Of equal importance, the application of the engineered enzyme is not limited to glucose sensors but may be used to detect DNA (and possibly other molecules) via electrochemical coupling.

REFERENCES

1. JG Hauge. Glucose dehydrogenase from *Bacterium antiratum*: an enzyme with a novel prosthetic group. J Biol Chem 239:3630–3639, 1964.
2. J Westerling, J Frank, JA Duine. The prosthetic group of methanol dehydrogenase from Hyphomicrobium X: electron spin resonance evidence for a quinone structure. Biochem Biophys Res Commun 87:719–724, 1979.
3. SA Salisbury, H Forrest, WBT Cruse, O Kennard. A novel coenzyme from bacterial primary alcohol dehydrogenases. Nature 280:843–844, 1979.
4. C Anthony. Methanol dehydrogenase in Gram-negative bacteria. In: V Davidson, ed. Principles and Applications of Quinoproteins. New York: Dekker, 1993, pp 17–45.
5. C Anthony. Quinoprotein-catalyzed reactions. Biochem J 320:697–711, 1996.
6. C Anthony. The structure and function of the PQQ-containing quinoprotein dehydrogenases. Prog Biophys Mol Biol 69:1–21, 1998.
7. C Anthony. Pyrroloquinoline quinone (PQQ) and quinoprotein enzymes. Antioxid Redox Signal 3:757–774, 2001.
8. JA Duine. PQQ and quinoprotein research—the first decade. Biofactors 2:87–94, 1989.
9. JA Duine. Quinoproteins: enzymes containing the quinonoid cofactor pyrroloquinoline quinone, topaquinone or tryptophan–tryptophyl quinone. Eur J Biochem 200:271–284, 1991.
10. JA Duine. The PQQ story. J Biosci Bioeng 88:231–236, 1999.
11. PM Goodwin, C Anthony. The biochemistry, physiology and genetics of PQQ and PQQ-containing enzymes. Adv Microb Physiol 40:1–80, 1998.
12. K Matsushita, O Adachi. Bacterial quinoproteins glucose dehydrogenase and alcohol dehydrogenase. In: V Davidson, ed. Principles and Applications of Quinoproteins. New York: Dekker, 1993, pp 245–273.
13. K Matsushita, H Toyama, M Yamada, O Adachi. Quinoproteins: structure, function, and biotechnological applications. Appl Microbiol Biotechnol 58:13–22, 2001.

14. WS McIntire. Quinoproteins. FASEB J 8:513–521, 1994.
15. BW Groen, MA van Kleef, JA Duine. Quinohaemoprotein alcohol dehydrogenase apoenzyme from *Pseudomonas testosteroni*. Biochem J 234:611–615, 1986.
16. H Toyama, A Fujii, K Matsushita, E Shinagawa, M Ameyama, O Adachi. Three distinct quinoprotein alcohol dehydrogenases are expressed when *Pseudomonas putida* is grown on different alcohols. J Bacteriol 177:2442–2450, 1995.
17. G Zarnt, T Schrader, JR Andreesen. Catalytic and molecular properties of the quinohemoprotein tetrahydrofurfuryl alcohol dehydrogenase from *Ralstonia eutropha* strain Bo. J Bacteriol 183:1954–1960, 2001.
18. M Shimao, K Ninomiya, O Kuno, N Kato, C Sakazawa. Existence of a novel enzyme, pyrroloquinoline quinone-dependent polyvinyl alcohol dehydrogenase, in bacterial symbiont, *Pseudomonas* sp. strain VM15C. Appl Environ Microbiol 51:268–275, 1986.
19. M Yasuda, A Cherepanov, JA Duine. Polyethylene glycol dehydrogenase activity of *Rhodopseudomonas acidophila* derives from a type I quinohaemoprotein alcohol dehydrogenase. FEMS Microbiol Lett 138:23–28, 1996.
20. F Kawai, H Yamanaka, M Ameyama, E Shinagawa, K Matsushita, O Adachi. Identification of the prosthetic group and further characterization of a novel enzyme, polyethylene-glycol dehydrogenase. Agric Biol Chem 49:1071–1076, 1985.
21. K Matsushita, H Toyama, O Adachi. Respiratory chain and bioenergetics of acetic acid bacteria. In: AH Rose, DW Tempest, eds. Advances in Microbial Physiology. Vol. 36. London: Academic Press, 1994, pp 247–301.
22. K Sode, K Matsumura, W Tsugawa, M Tanaka. Isolation of a marine bacterial pyrroloquinoline quinone-dependent glucose dehydrogenase. J Mar Biotechnol 2:214–218, 1995.
23. D Moonmangmee, Y Fujii, H Toyama, G Theeragool, N Lotong, K Matsushita, O Adachi. Purification and characterization of membrane-bound quinoprotein cyclic alcohol dehydrogenase from Gluconobacter frateurii CHM 9. Biosci Biotechnol Biochem 65:2763–2772, 2001.
24. O Adachi, Y Fujii, MF Ghaly, H Toyama, E Shinagawa, K Matsushita. Membrane-bound quinoprotein D-arabitol dehydrogenase of *Gluconobacter suboxydans* IFO 3257: a versatile enzyme for the oxidative fermentation of various ketoses. Biosci Biotechnol Biochem 65:2755–2762, 2001.
25. JA Zahn, DJ Bergmann, JM Boyd, RC Kunz, AA DiSpirito. Membrane-associated quinoprotein formaldehyde dehydrogenase from *Methylococcus capsulatus* Bath. J Bacteriol 183:6832–6840, 2001.
26. DJ Hopper, J Rogozinski. Redox potential of the haem group in the quinocytochrome, lupanine hydroxylase, an enzyme located in the periplasm of a *Pseudomonas* sp. Biochim Biophys Acta 1383:160–164, 1998.
27. ES Choi, EH Lee, SK Rhee. Purification of membrane-bound sorbitol dehydrogenase from *Gluconobacter suboxydans*. FEMS Microbiol Lett, 12545–12550, 1995. AQ2
28. A Asakura, T Hoshino. Isolation and characterization of a new quinoprotein

dehydrogenase, L-sorbose/L-sorbosone dehydrogenase. Biosci Biotech Biochem 62:469–478, 1999.

29. MAG van Kleef, JA Duine. Bacterial NAD(P)-independent quinate dehydrogenase is a quinoprotein. Arch Microbiol 150:32–36, 1988.
30. AS Vangnai, DJ Arp, LA Sayavedra-Soto. Two distinct alcohol dehydrogenases participate in butane metabolism by *Pseudomonas butanovora*. J Bacteriol 184:1916–1924, 2002.
31. M Ameyama, E Shinagawa, K Matsushita, O Adachi. Solubilization, purification and properties of membrane-bound glycerol dehydrogenase from *Gluconobacter industrius*. Agric Biol Chem 49:1001–1010, 1985.
32. C Anthony, LJ Zatman. Isolation and properties of *Pseudomonas* sp. M27. Biochem J 92:609–614, 1964.
33. C Anthony, LJ Zatman. The methanol-oxidizing enzyme of *Pseudomonas* sp. M27. Biochem J 92:614–621, 1964.
34. C Anthony. The bacterial oxidation of methane and methanol. Adv Microb Physiol 27:113–210, 1986.
35. DN Nunn, DJ Day, C Anthony. The second subunit of methanol dehydrogenase of *Methylobacterium extorquens* AM1. Biochem J 260:857–862, 1989.
36. ZX Xia, WW Dai, JP Xiong, ZP Hao, VL Davidson, S White, FS Mathews. The 3-dimensional structures of methanol dehydrogenase from 2 methylotrophic bacteria at 2.6Å resolution. J Biol Chem 267:22289–22297, 1992.
37. M Paori. Protein folds propelled by diversity. Prog Biophys Mol Biol 76:103–130, 2001.
38. H Görisch, M Rupp. Quinoprotein ethanol dehydrogenase from Pseudomonas. Antonie van Leeuwenhoek 56:35–45, 1989.
39. T Keitel, A Diehl, T Knaute, JJ Stezowski, W Höhne, H Görisch. X-ray structure of the quinoprotein ethanol dehydrogenase from *Pseudomonas aeruginosa*: basis of substrate specificity. J Mol Biol 297:961–974, 2000.
40. A Oubrie, HJ Rozeboom, KH Kalk, EG Huizinga, BW Dijkstra. Crystal structure of quinohemoprotein alcohol dehydrogenase from *Comamonas testosteroni* structural basis for substrate oxidation and electron transfer. J Biol Chem 277:3727–3732, 2002.
41. O Adachi, K Tayama, E Shinagawa, K Matsushita, M Ameyama. Purification and characterization of particulate alcohol dehydrogenase from *Gluconobacter suboxydans*. Agric Biol Chem 42:2045–2056, 1978.
42. O Adachi, E Miyagawa, E Shinagawa, K Matsushita, M Ameyama. Purification and properties of particulate alcohol dehydrogenase from *Acetobacter aceti*. Agric Biol Chem 42:2331–2340, 1978.
43. A Ramanavicius, K Habermüller, E Csöregi, V Laurinavicius, W Schuhmann. Polypyrrole-entrapped quinohemoprotein alcohol dehydrogenase. Evidence for direct electron transfer via conducting-polymer chains. Anal Chem 71:3581–3586, 1999.
44. K Matsushita, E Shinagawa, O Adachi, M Ameyama. Quinoprotein D-glucose dehydrogenase of the *Acinetobacter calcoaceticus* respiratory chain: membrane-bound and soluble forms are different molecular species. Biochemistry 28:6276–6280, 1989.

45. AM Cleton-Jansen, N Goosen, TJ Wenzel, P van de Putte. Cloning of the gene encoding quinoprotein glucose dehydrogenase from *Acinetobacter calcoaceticus*: evidence for the presence of a second enzyme. J Bacteriol 170:2121–2125, 1988.
46. AM Cleton-Jansen, N Goosen, G Odle, P van de Putte. Nucleotide sequence of the gene coding for quinoprotein glucose dehydrogenase from *Acinetobacter calcoaceticus*. Nucleic Acids Res 16:6228, 1988.
47. AM Cleton-Jansen, N Goosen, O Fayet, P van de Putte. Cloning, mapping, and sequencing of the gene encoding *Escherichia coli* quinoprotein glucose dehydrogenase. J Bacteriol 172:6308–6315, 1990.
48. K Matsushita, Y Ohno, E Shinagawa, O Adachi, M Ameyama. Membrane-bound, electron transport-linked, D-glucose dehydrogenase of *Pseudomonas fluorescens*. Interaction of the purified enzyme with ubiquinone or phospholipid. Agric Biol Chem 46:1007–1011, 1982.
49. M Beardmore-Gray, C Anthony. The oxidation of glucose by *Acinetobacter calcoaceticus*: interaction of the quinoprotein glucose dehydrogenase with the electron transport chain. J Gen Microbiol 132:1257–1268, 1986.
50. AM Cleton-Jansen, S Dekker, P van de Putte, N Goosen. A single amino acid substitution changes the substrate specificity of quinoprotein glucose dehydrogenase in *Gluconobacter oxydans*. Mol Gen Genet 229:206–212, 1991.
51. CJ Pujol, CI Kado. gdhB, a gene encoding a second quinoprotein glucose dehydrogenase in *Pantoea citrea*, is required for pink disease of pineapple. Microbiology 145:1217–1226, 1999.
52. AH Goldstein, PU Krishnaraj, Submitted for publication (GenBank accession number: AF441442)
53. GE Cozier, C Anthony. Structure of quinoprotein glucose dehydrogenase of *Escherichia coli* modeled on that of methanol dehydrogenase from *Methylobacterium extorquens*. Biochem J 312:679–685, 1995.
54. AB Witarto, S Obuchi, M Narita, K Sode. Secondary structure study of pyrroloquinoline quinone glucose dehydrogenase. J Biochem Mol Biol Biophys 2:209–213, 1999.
55. M Yamada, K Sumi, K Matsushita, O Adachi, Y Yamada. Topological analysis of quinoprotein glucose dehydrogenase in *Escherichia coli* and its ubiquinone-binding site. J Biol Chem 268:12812–12817, 1993.
56. K Sode, H Sano. Glu742 substitution to Lys enhances the EDTA tolerance of *Escherichia coli* PQQ glucose dehydrogenase. Biotechnol Lett 16:455–460, 1994.
57. K Sode, K Watanabe, S Ito, K Matsumura, T Kikuchi. Thermostable chimeric PQQ glucose dehydrogenase. FEBS Lett 364:325–327, 1995.
58. K Sode, H Yoshida, K Matsumura, T Kikuchi, M Watanabe, N Yasutake, S Ito, H Sano. Elucidation of the region responsible for EDTA tolerance in PQQ glucose dehydrogenases by constructing *Escherichia coli* and *Acinetobacter calcoaceticus* chimeric enzymes. Biochem Biophys Res Commun 211:268–273, 1995.
59. K Sode, K Kojima. Improved substrate specificity and dynamic range for glucose measurement of *Escherichia coli* PQQ glucose dehydrogenase by site directed mutagenesis. Biotechnol Lett 19:1073–1077, 1997.
60. K Sode, H Yoshida. Construction and characterization of a chimeric *Escherichia*

coli PQQ glucose dehydrogenase (PQQGDH) with increased EDTA tolerance. Denki Kagaku 65:444–451, 1997.

61. H Yoshida, K Sode. Thr424 to Asn substitution alters bivalent metal specificity of pyrroloquinoline quinone glucose dehydrogenase. J Biochem Mol Biol Biophys 1:89–93, 1997.
62. J Okuda, H Yoshida, K Kojima, M Himi, K Sode. The role of conserved His775/781 in membrane-binding PQQ glucose dehydrogenase of *Escherichia coli* and *Acinetobacter calcoaceticus*. J Biochem Mol Biol Biophys 4:415–422, 2000.
63. H Yoshida, K Kojima, AB Witarto, K Sode. Engineering a chimeric pyrroloquinoline quinone glucose dehydrogenase: improvement of EDTA tolerance, thermal stability and substrate specificity. Protein Eng 12:63–70, 1999.
64. LD Elias, M Tanaka, H Izu, K Matsushita, O Adachi, M Yamada. Functions of amino acid residues in the active site of *Escherichia coli* PQQ-containing quinoprotein glucose dehydrogenase. J Biol Chem 275:7321–7326, 2000.
65. LD Elias, M Tanaka, M Sakai, M Toyama, K Matsushita, O Adachi, M Yamada. C-terminal periplasmic domain of *Escherichia coli* quinoprotein glucose dehydrogenase transfers electrons to ubiquinone. J Biol Chem 276:48356–48361, 2001.
66. GE Cozier, RA Salleh, C Anthony. Characterization of the membrane quinoprotein glucose dehydrogenase from *Escherichia coli* and characterization of a site-directed mutant in which histidine-262 has been changed to tyrosine. Biochem J 340:639–647, 1999.
67. AM Cleton-Jansen, N Goosen, K Vink, P van de Putte. Cloning, characterization and DNA sequencing of the gene encoding the Mr 50,000 quinoprotein glucose dehydrogenase from *Acinetobacter calcoaceticus*. Mol Gen Genet 217: 430–436, 1989.
68. A Oubrie, HJ Rozeboom, KH Kalk, JA Duine, BW Dijkstra. The 1.7Å crystal structure of the apo-form of the soluble quinoprotein glucose dehydrogenase from *Acinetobacter calcoaceticus* reveals a novel internal conserved sequence repeat. J Mol Biol 289:319–333, 1999.
69. K Sode, T Ohtera, M Shirahane, AB Witarto, S Igarashi, H Yoshida. Increasing the thermal stability of the water-soluble pyrroloquinoline quinone glucose dehydrogenase by single amino acid replacement. Enzyme Microb Technol 26: 491–496, 2000.
70. P Dokter, J Frank, JA Duine. Purification and characterization of quinoprotein glucose dehydrogenase from *Acinetobacter calcoaceticus* L.M.D.79.41. Biochem J 239:163–167, 1986.
71. S Igarashi, T Ohtera, H Yoshida, AB Witarto, K Sode. Construction and characterization of mutant water-soluble PQQ glucose dehydrogenases with altered Km value—site-directed mutagenesis studies on the putative active site. Biochem Biophys Res Commun 264:820–824, 1999.
72. A Oubrie, HJ Rozeboom, KH Kalk, AJJ Olsthoorn, JA Duine, BW Dijkstra. Structure and mechanism of soluble quinoprotein glucose dehydrogenase. EMBO J 18:5187–5194, 1999.
73. LC Clark, C Lyons. Electrode systems for continuous monitoring in vascular surgery. Ann NY Aead Sci 102:29–45, 1962.

74. AEG Cass, DG Francis, HAO Hill, WJ Aston, IJ Higgins, EV Plotkin, LD Scott, APF Turner. Ferrocene-mediated enzyme electrode for amperometric determination of glucose. Anal Chem 56:667–671, 1984.
75. DR Matthews, RR Holman, E Brown, J Steemson, A Watson, S Hughes, D Scott. Pen sized digital 30-second blood glucose meter. Lancet 4:778–779, 1987.
76. Y Degani, A Heller. Direct electrical communication between chemically modified enzymes and metal electrodes. 1. Electron transfer from glucose oxidase to metal electrodes via electron relays, bound covalently to the enzyme. J Phys Chem 91:1285–1288, 1987.
77. EJ D'Costa, IJ Higgins, APF Turner. Quinoprotein glucose dehydrogenase and its application in an amperometric glucose sensor. Biosensors 2:71–87, 1986.
78. L Ye, M Hammerle, AJJ Olsthoorn, W Schuhmann, HL Schmidt, JA Duine, A Heller. High current density "wired" quinoprotein glucose dehydrogenase electrode. Anal Chem 65:238–241, 1993.
79. GJ Kost, HT Vu, JH Lee, P Bourgeois, FL Kiechle, C Martin, SS Miller, AO Okorodudu, JJ Podczasy, R Webster, KJ Whitlow. Multicenter study of oxygen-insensitive handheld glucose point-of-care testing in critical care/hospital/ambulatory patients in the United States and Canada. Crit Care Med 26:581–590, 1998.
80. H Yoshida, T Iguchi, K Sode. Construction of multi-chimeric pyrroloquinoline quinone glucose dehydrogenase with improved enzymatic properties and application in glucose monitoring. Biotechnol Lett 22:1505–1510, 2000.
81. Y Takahashi, S Igarashi, Y Nakazawa, W Tsugawa, K Sode. Construction and characterization of glucose enzyme sensor employing engineered water soluble PQQ glucose dehydrogenase with improved thermal stability. Electrochemistry 68:907–911, 2000.
82. JA Duine, J Frank, JA Jongejan. Detection and determination of pyrroloquinoline quinone, the coenzyme of quinoproteins. Anal Biochem 133:443–446, 1983.
83. M Yamada, H Inbe, M Tanaka, K Sumi, K Matsushita, O Adachi. Mutant isolation of the *Escherichia coli* quinoprotein glucose dehydrogenase and analysis of crucial residues Asp-730 and His-775 for its function. J Biol Chem 273:22021–22027, 1998.
84. K Sode, S Igarashi, A Morimoto, H Yoshida. In press.
85. JM Slauch, TJ Silhavy. Genetic fusions as experimental tools. Methods Enzymol 204:213–248, 1991.
86. K Sode, M Shirahane, H Yoshida. Construction and characterization of a linked-dimeric pyrroloquinoline quinone glucose dehydrogenase. Biotechnol Lett 21:707–710, 1999.
87. S Igarashi, K Sode. Submitted for publication.
88. K Sode, AB Witarto, K Watanabe, K Noda, S Ito, W Tsugawa. Over expression of PQQ glucose dehydrogenase in *Escherichia coli* under holoenzyme forming condition. Biotechnol Lett 16:1265–1268, 1994.
89. K Sode, K Ito, AB Witarto, K Watanabe, H Yoshida, P Postma. Increased production of recombinant pyrroloquinoline quinone (PQQ) glucose dehydrogenase by metabolically engineered *Escherichia coli* strain capable of PQQ biosynthesis. J Biotechnol 49:239–243, 1996.

90. K Kojima, AB Witarto, K Sode. The production of soluble pyrroloquinoline quinone glucose dehydrogenase by *Klebsiella pneumoniae*, the alternative host of PQQ enzymes. Biotechnol Lett 22:1343–1347, 2000.
91. H Yoshida, N Araki, A Tomisaka, K Sode. Secretion of water soluble pyrroloquinoline quinone glucose dehydrogenase by recombinant *Pichia pastoris*. Enzyme Microb Technol 13:312–318, 2002.
92. T Yamazaki, K Kojima, K Sode. Extended-range glucose sensor employing engineered glucose dehydrogenases. Anal Chem 72:4689–4693, 2000.
93. H Yoshida, T Iguchi, K Sode. Construction of multi-chimeric pyrroloquinoline quinone glucose dehydrogenase with improved enzymatic properties and application in glucose monitoring. Biotechnol Lett 22:1505–1510, 2000.
94. K Ikebukuro, Y Kohiki, K Sode. Amperometric DNA sensor using the pyrroloquinoline quinone glucose dehydrogenase-avidin conjugate. In press.